

Label-free optical detection of small-molecule compound microarrays immobilized on solid support using macromolecular scaffolds and subsequent protein binding reactions

Y.S. Sun^a, J.P. Landry^a, Y.Y. Fei^a, X.D. Zhu^a, J.T. Luo^b, X.B. Wang^b, K.S. Lam^b

^aDepartment of Physics, University of California at Davis, Davis, CA 95616;

^bDivision of Hematology and Oncology, Department of Internal Medicine, University of California at Davis, Sacramento, CA 95817

ABSTRACT

Small-molecule microarrays composed of tens of thousands of distinct synthetic molecules, natural products, and their combinations/modifications provide a high-throughput platform for studying protein-ligand interactions. Immobilization of small molecule compounds on solid supports remains a challenge as widely varied small molecules generally lack unique chemical groups that readily react with singly or even multiply functionalized solid support. We explored two strategies for immobilizing small molecule compounds on epoxy-functionalized glass surface using primary-amine-containing macromolecular scaffolds: bovine serum albumin (BSA) and amine-modified poly-vinyl alcohol (PVA). Small molecules with N-hydroxysuccinimide (NHS) groups were conjugated to BSA or amine-modified PVA. Small-molecule-BSA conjugates and small-molecule-PVA conjugates were subsequently immobilized on epoxy-functionalized glass slides through amine-epoxy reactions. Using an oblique-incidence reflectivity difference (OI-RD) scanning microscope as a label-free detector, we performed a comparative study of the effectiveness of BSA and PVA as macromolecular scaffolds for anchoring small molecule compounds in terms of conjugation efficiency, surface immobilization efficiency, effect of the scaffold on end-point and kinetics of subsequent binding reactions with protein probes.

Keywords: small-molecule microarrays, label-free detection, ellipsometry, oblique-incidence reflectivity difference, OI-RD, kinetics, equilibrium dissociation constant, Langmuir two-site model, protein-ligand interaction

1. INTRODUCTION

Small-molecule microarrays (SMMs) composed of synthetic and natural compounds including peptides provide a high-throughput platform for studying protein functions and investigating particular protein ligands¹. By screening SMMs against cell lysates, normal or diseased human sera, and even bacteria or viruses, one can explore a diverse variety of protein-ligand interactions and discover useful inhibitors² and thus drug candidates³ that activate or deactivate specific protein functions. Due to large structural diversity of small molecules from a wide range of synthetic and natural sources and yet for lack of a common chemical residue that one can use as a universal surface anchor, it remains a formidable challenge to efficiently immobilize these small molecules on specially functionalized solid support. One strategy useful for some of the synthetic compound libraries is to attach a common surface anchoring molecular scaffold to the compounds so that such a compound library can be immobilized on a suitably functionalized solid support with a more or less uniform efficiency. Typically to minimize the effect of attaching a molecular scaffold to small molecule compounds on the functionality of the compounds, specific linkages are often introduced between the small molecules and the scaffold. Many efforts have been made in the preparation of SMMs, including using ketone-modified macromolecular scaffolds⁴, immobilization of hydrazide-linked substances on epoxide-coated glass surfaces⁵, non-specific isocyanate-mediated surface immobilization⁶, photoactivated capture on gold surfaces for SPR imaging⁷, and immobilization of biotinylated one-bead one-compound (OBOC) combinatorial library on streptavidin-functionalized slides⁸. We have explored a different strategy for immobilizing synthetic compounds on epoxy-functionalized glass surface using primary-amine-containing macromolecular scaffolds as surface anchors: bovine serum albumin (BSA) and amine-modified poly-vinyl alcohol (PVA).

Besides surface immobilization, developing non-intrusive techniques for interrogating small-molecule compound microarray and subsequent protein binding reactions is necessary and challenging at the same time. Fluorescence-based techniques have been widely used in application to microarray detection mainly for their superior sensitivity, low

excess of amino groups on the scaffold for the immobilization onto the epoxy glass slide during the microarray printing. A 10% NH₂-derived PVA is used to increase the ability and feasibility in loading small molecules.

2.1.2 Conjugation of small molecules onto macromolecules

For performance evaluation, we used biotin molecules as test small molecule targets. Biotin molecules were coupled onto amino functionalized macromolecules (amino-PVA or BSA) by introduction of 4% biotin to 10% NH₂-derived PVA (or BSA): 0.5 mL of NHS ester of biotin (0.23 μmol) solution in DMSO was added into 5 mL solution of the amino-PVA (NH₂: OH = 1: 9, 250 mg, 0.56 μmol of -NH₂) in 0.1 M NaHCO₃ and rotated in a plastic tube overnight. Biotinylated PVA was precipitated by addition of 25 mL of ethanol, filtered and washed with ethanol and acetonitrile 3 times, respectively, and then dissolved in 5 mL of pure water and lyophilized. For biotin-PVA, 1%, 2% or 4% of biotin was introduced. For BSA, biotin molecules in different molar ratios (5, 10, 20 or 40) were introduced to BSA during conjugation. Only a fraction of 35 surface amine groups on a BSA molecule were used to conjugate biotin molecules, and the remaining amine groups were available to subsequent surface immobilization on epoxy-functionalized glass slides.

2.2 Preparation of small molecule microarrays

Small-molecule conjugates, biotin-BSA and biotin-PVA, were dissolved in 1×PBS (pH 7.4, 0.22 μm filtered) and further diluted into a set of solutions with concentrations decreasing successively by a factor of 0.5 from 18 μM to 0.14 μM for BSA conjugates and from 77 μM to 0.6 μM for PVA conjugates. The solutions were printed into microarrays on an epoxy-functionalized glass slide with a micro-contact-printing arrayer (OmniGrid100, Genomic Solutions, Ann Arbor, MI). The epoxy-coated glass slides were purchased from CEL Associates (Pearland, TX). The microarray consisted of biotin-BSA (with 5×, 10×, 20× and 40× loadings) and biotin-PVA (with 1%, 2% and 4% loadings) in titration series. We also printed BSA at 18 μM in 1×PBS and PVA of 77 μM (13 kDa, 10% NH₂-derived) also in 1×PBS, both without conjugated biotin molecules as negative controls. The microarray-bearing slides were stored as printed in a slide box for at least 24 hours before further processing. Before optical measurements a printed glass slide was immersed in 1×PBS buffer overnight to remove excess unbound targets and buffer precipitates.

2.3 Setup and working principles of an OI-RD scanning microscope

In Fig. 2, we show the arrangement of an OI-RD scanning microscope. Let $r_{p0} = |r_{p0}| \exp(i\Phi_{p0})$ and $r_{s0} = |r_{s0}| \exp(i\Phi_{s0})$ be the respective reflectivity for p- and s-polarized light from a “bare” solid substrate surface. Let $r_p = |r_p| \exp(i\Phi_p)$ and $r_s = |r_s| \exp(i\Phi_s)$ be the reflectivity when a layer of molecules is added to the surface or when the surface is modified (e.g., conformational change of a pre-existing molecular layer) as a result of the biochemical event. In our scanning optical microscope, we measure $\Delta_p - \Delta_s \equiv (r_p - r_{p0})/r_{p0} - (r_s - r_{s0})/r_{s0}$ as the contrast^{11,12}. The information on the newly added surface-bound molecular is related to $\Delta_p - \Delta_s$ by¹³

$$\Delta_p - \Delta_s \cong -i \left[\frac{4\pi\epsilon_s (\tan \phi_{inc})^2 \cos \phi_{inc}}{\epsilon_0^{1/2} (\epsilon_s - \epsilon_0) (\epsilon_s / \epsilon_0 - (\tan \phi_{inc})^2)} \right] \frac{(\epsilon_d - \epsilon_s)(\epsilon_d - \epsilon_0) \Theta \left(\frac{d}{\lambda} \right)}{\epsilon_d} \quad (1)$$

ϕ_{inc} is the incidence angle. ϵ_0 , ϵ_d , and ϵ_s are the optical dielectric constants of the ambient, the surface-bound molecular layer, and the substrate, respectively. d is the thickness of the molecular layer. Θ is the coverage of the layer, defined as the ratio of the surface area covered by the molecular layer to the total available surface area. Changes in mass density, chemical composition, and conformation are reflected by the corresponding changes in ϵ_d . At the interface of two transparent media (ϵ_0 and ϵ_s being real), a non-absorbing biomolecular layer with ϵ_d only yields $\text{Im}\{\Delta_p - \Delta_s\}$ or the differential phase change,

$$\text{Im}\{\Delta_p - \Delta_s\} = - \left[\frac{4\pi\epsilon_s (\tan \phi_{inc})^2 \cos \phi_{inc}}{\epsilon_0^{1/2} (\epsilon_s - \epsilon_0) (\epsilon_s / \epsilon_0 - (\tan \phi_{inc})^2)} \right] \frac{(\epsilon_d - \epsilon_s)(\epsilon_d - \epsilon_0) \Theta \left(\frac{d}{\lambda} \right)}{\epsilon_d} \quad (2)$$

This is what we monitor when detecting binding reactions of proteins with small molecule microarrays. Up to an incidence-angle-dependent factor, $\Delta_p - \Delta_s$ is same as the corresponding surface-plasmon resonance (SPR) angle shift, $\delta\theta_{\text{SPR}} \approx (3\pi d/\lambda)(\epsilon_d - \epsilon_0)/\epsilon_d$ ¹⁴ when a molecular film of thickness d and optical dielectric constant ϵ_d is sandwiched between a gold substrate and an aqueous ambient with optical constant ϵ_0 .

The procedures for obtaining $\Delta_p - \Delta_s$ have been described in details previously¹⁵ and will not be repeated here. In the present study, we used a 60° prism and index-matching fluid to form a good optical contact with one side of a glass slide. The other side of the slide was covered with printed small molecule microarrays and in contact with an aqueous solution. The illumination optical beam (He-Ne laser at wavelength $\lambda = 633$ nm) with a diameter of 10-mm entered one side of the prism and is focused (with a cylindrical lens) to a 15- $\mu\text{m} \times 10$ -mm line on the microarray-bearing surface along y-axis and then totally reflected from the surface. The reflected beam from a 15- $\mu\text{m} \times 3$ -mm line segment in the center of the illuminated region exited the other side of the prism. With a 10 \times objective, the beam was imaged onto a 50-mm long 152-element, photodiode detector so that each photodiode detected the light from a 20-micron segment of the illuminated line. We acquired an image of a printed microarray by electronically interrogating 152 photodiode elements in series for y-scan and mechanically moving the sample-holding stage along x-axis for x-scan. The pixel dimension was thus 20 $\mu\text{m} \times 20$ μm . To acquire real-time binding (association-dissociation) curves from surface-immobilized molecular targets, we selected one pixel from each of the printed targets and one pixel from the unprinted region adjacent to the target as the reference and measured the OI-RD signals from these pixels only at a fixed time interval much smaller than the characteristic time constants of the reactions. To remove the drift in the optical detection system, we took the difference between the OI-RD signal from the target pixel and the OI-RD signal from the neighboring reference pixel.

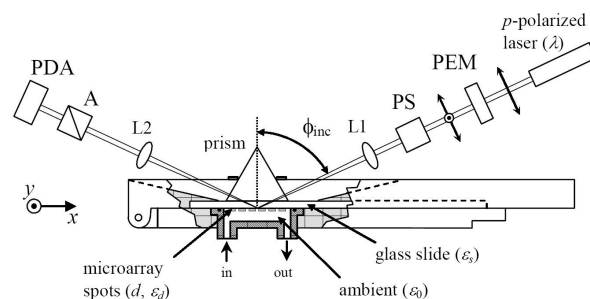


Fig. 2. Sketch of a scanning oblique-incidence reflectivity difference (OI-RD) microscope for in-situ detection of binding reactions of liquid-phase protein probes with a surface-immobilized small molecule microarray. It employs the total internal reflection geometry for illumination, and a combination of a 152-element photo-diode array (PDA) detector for y-scan and a mechanical stage for x-scan. PEM: photoelastic modulator that periodically changes the polarization of the illumination laser. PS: variable phase-shifter. L1: cylindrical lens for line illumination. L2: 10 \times objective lens that images the illuminated line on the sample surface onto PDA. A: polarization analyzer.

2.4 Reaction conditions of small molecule microarrays

After the printed slide was washed overnight (see section 2.2), it was assembled between the prism and the flow cell. A few μL of index matching fluid with refractive index $n = 1.52$ was pipetted between the slide and the prism to ensure total internal reflection occurring at the microarray-bearing surface. The flow cell (volume ~ 400 μL) was connected to a syringe pump and a 6-way valve for switching between 1 \times PBS buffer and reagents. Then the slide was washed again with a flow of 1 \times PBS at a rate of 30 mL/min twice, blocked with BSA (7.6 μM in 1 \times PBS) for 10 min, and then washed with fresh 1 \times PBS for 5 min. It was subsequently reacted with a selected protein probe solution. For real-time measurements, we first filled the flow cell with the desired protein solution quickly at a flow rate of 30 mL/min and then slowed down to 0.05 mL/min during the association phase. To observe the dissociation, we quickly replaced the protein solution with 1 \times PBS at a flow rate of 30 mL/min first and then slowed down to 0.05 mL/min during the dissociation phase. The BSA and monovalent mouse IgG fragments against biotin anti-biotin as protein probes were purchased from Jackson ImmunoResearch Laboratories (West Grove, PA). Both were diluted in 1 \times PBS buffer.

3. RESULTS AND DISCUSSION

3.1 Label-free detection of end-points of biotin-antibody reactions

In Fig. 3(a), we show the OI-RD image in $\text{Im}\{\Delta_p - \Delta_s\}$ of a 7 \times 10 microarray composed of biotin-BSA, biotin-PVA, blank BSA and blank PVA on an epoxy-coated glass slide after the excess printed materials were washed off. Different columns correspond to different conjugates; different rows correspond to different printing concentrations as indicated.

The microarray was then blocked with BSA to quench unreacted epoxy groups. BSA does not react with mouse antibody against biotin. The BSA blocked microarray was then reacted with the mouse anti-biotin antibody at a concentration of 87 nM for 4 h. The OI-RD image afterward was shown in Fig. 3(b). Optical signals $\text{Im}\{\Delta_p - \Delta_s\}$ increased at all spots containing biotin targets, even those printed at low target concentrations. Fig. 3(c) shows the differential image that highlights the quantitative effect of the reaction between the mouse antibody and biotin targets. Blank BSA and blank PVA indeed serve as negative controls as they did not change when exposed to the mouse anti-biotin antibodies.

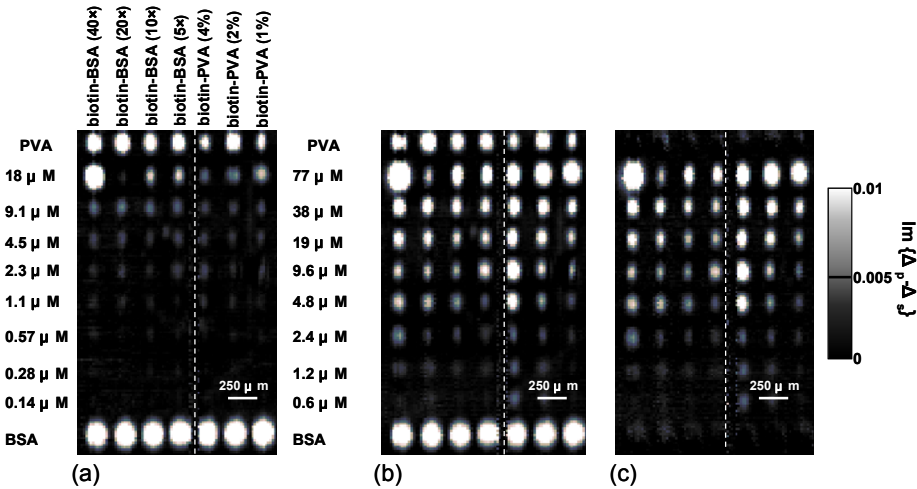


Fig. 3 OI-RD images in $\text{Im}\{\Delta_p - \Delta_s\}$ of a biotin-BSA and biotin-PVA microarray (separated by a dashed line) with different conjugation loadings and printing concentrations, along with blank BSA and blank PVA included as negative controls. (a) Image of the microarray after washing, but before blocking. (b) Image of the microarray after reacting with anti-biotin. (c) Change in OI-RD image due to mouse antibody binding to biotin targets by subtracting the image after blocking from the image after reaction.

To quantify the amount of mouse antibody probes bound to the target-covered surface, we reexamine Eq. (2). The coverage Θ and the thickness d of the biomolecular layer are related to the surface mass density Γ and the volume mass density ρ of the surface-bound by $\Gamma = \Theta d \rho$. Rearranging Eq. (2) and putting in numerical values such as $\phi_{\text{inc}} = 65^\circ$, $\epsilon_s = 2.307$ for the glass slide, $\epsilon_0 = 1.788$ for the aqueous buffer, $\epsilon_d = 2.031$ for proteins in solution, $\lambda = 633 \text{ nm}$ for the He-Ne laser, and $\rho_{\text{protein}} = 1.35 \text{ g/cm}^3$, we arrive at

$$\Gamma = (1.85 \times 10^{-4} \text{ g/cm}^2) \text{Im}\{\Delta_p - \Delta_s\} \quad (3)$$

From Eq. (3), we convert $\text{Im}\{\Delta_p - \Delta_s\}$ signal into the surface mass density Γ of the captured protein layer. Fig. 4(a) and 4(b) plot changes in $\text{Im}\{\Delta_p - \Delta_s\}$ and Γ versus printing concentration. For mouse anti-biotin antibody modeled as ellipsoid, the surface mass density of a “side-on” monolayer with long axis parallel to the surface and packed in form of a square-lattice is about $2.5 \times 10^{-7} \text{ g/cm}^2$, and that of a “end-on” monolayer” (with long axis perpendicular to the surface and again packed in square lattice) is about $13 \times 10^{-7} \text{ g/cm}^2$.¹⁶ Two dashed lines corresponding to these two values are drawn for comparison. Panel (a) shows the efficiency of biotin conjugation to BSA at different molar ratios during conjugation. There are two general trends: the amount of captured mouse anti-biotin antibodies increases with printing concentration, and spots printed with biotin-BSA conjugates made with biotin-to-BSA molar ratio of 40 (i.e., 40 \times) give largest signal. For example, at a printing concentration of 9 μM , the surface mass density of captured antibodies for 40 \times biotin-BSA is about $33 \times 10^{-7} \text{ g/cm}^2$, while for biotin-BSA conjugates made with biotin-to-BSA molar ratio of 20, 10, and 5 (i.e., 20 \times , 10 \times and 5 \times) the signals are only about $18 \times 10^{-7} \text{ g/cm}^2$. Regardless of biotin-to-BSA molar ratio or loading, we easily have more than a “side-on” monolayer of the captured mouse antibodies bound as long as the printing concentration is higher than 0.3 μM . Panel (b) represents PVA conjugates, where the amount of captured antibodies increases when either printing concentration or biotin-to-PVA molar ratio loading increases. For example, at a printing concentration of 19 μM , the surface mass densities are about 29, 19 and $14 \times 10^{-7} \text{ g/cm}^2$ for 4%, 2% and 1% biotin-PVA,

respectively. Again, the surface mass density can be larger than that of a “side-on” or “end-on” monolayer when the printing concentration is high enough.

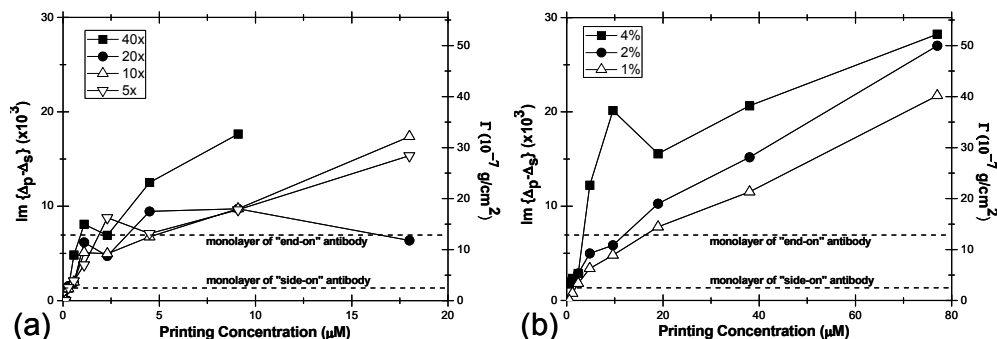


Fig. 4 Changes in $\text{Im}\{\Delta_p - \Delta_s\}$ and surface mass density Γ due to anti-biotin mouse antibody binding to surface-bound biotin targets as a function of target printing concentration. (a) Biotin-BSA conjugates with different loadings (biotin-to-BSA molar ratios). (b) Biotin-PVA conjugates with different loadings (biotin-to-PVA molar ratios). The dashed lines mark the values of a full “side-on” and a full “end-on” monolayer of mouse antibodies.

3.2 Real-time binding kinetics of protein-ligand reactions

In Fig. 5, we show the binding curves for reactions of anti-biotin with surface-immobilized biotin conjugates: (a) 40× biotin-BSA; (b) 20× biotin-BSA; (c) 10× biotin-BSA; (d) 5× biotin-BSA; (e) 4% biotin-PVA; (f) 1% biotin-PVA. Probe concentrations of 480, 240, 80 and 27 nM were used. To solution-phase protein probes, the surface-immobilized conjugated small molecule targets are better characterized by having more than one type. This is because the amine residues on BSA or PVA that are commissioned for small molecule conjugation are expectedly situated in different physical or stereo-chemical environments and small-molecule-BSA or small-molecule-PVA conjugates can assume different “orientations” when immobilized on an epoxy-coated surface^{10,17}. The binding curves shown in Fig. 5 were indeed better described by a two-site Langmuir reaction kinetic model. In this model, the optical signal is expected to vary as¹⁰

$$\text{Im}\{\Delta_p - \Delta_s\} = \gamma \left\{ \frac{N_1^{(0)} k_{on}^{(1)} [c]}{k_{on}^{(1)} [c] + k_{off}^{(1)}} \left(1 - e^{-(k_{on}^{(1)} [c] + k_{off}^{(1)}) t} \right) + \frac{N_2^{(0)} k_{on}^{(2)} [c]}{k_{on}^{(2)} [c] + k_{off}^{(2)}} \left(1 - e^{-(k_{on}^{(2)} [c] + k_{off}^{(2)}) t} \right) \right\} \quad (0 < t < t_0) \quad (4)$$

$$\text{Im}\{\Delta_p - \Delta_s\} = \gamma \left\{ \begin{aligned} & \frac{N_1^{(0)} k_{on}^{(1)} [c]}{k_{on}^{(1)} [c] + k_{off}^{(1)}} \left(1 - e^{-(k_{on}^{(1)} [c] + k_{off}^{(1)}) t_0} \right) e^{-(k_{off}^{(1)}) (t - t_0)} \\ & + \frac{N_2^{(0)} k_{on}^{(2)} [c]}{k_{on}^{(2)} [c] + k_{off}^{(2)}} \left(1 - e^{-(k_{on}^{(2)} [c] + k_{off}^{(2)}) t_0} \right) e^{-(k_{off}^{(2)}) (t - t_0)} \end{aligned} \right\} \quad (t > t_0) \quad (5)$$

where $N_1^{(0)}$ and $N_2^{(0)}$ are the respective numbers of available targets at Type-1 and Type-2 sites per unit area. $t_0 > 0$ is the time when the protein probe solution is replaced with 1×PBS and the dissociation proceeds alone. For each set of association-dissociation curves in Fig. 5, we performed a global fitting using Eq. (4) and (5) with $k_{on}^{(1)}$, $k_{off}^{(1)}$, $k_{on}^{(2)}$, $k_{off}^{(2)}$, $N_1^{(0)}/(N_1^{(0)} + N_2^{(0)}) \equiv \theta^{(1)}$ and $N_2^{(0)}/(N_1^{(0)} + N_2^{(0)}) \equiv \theta^{(2)}$ as the global fitting parameters. The equilibrium dissociation constant is given by $K_D = k_{off}/k_{on}$. For PVA, the binding curves were fitted better if we let the coverages of two sites be local fitting parameters instead of global parameters such that for each curve within a set these parameters were allowed to vary. This is not unreasonable since PVA is a long polymer and when printed at different times the immobilized polymers may very well assume different configurations. Fitting parameters are listed in Table 1. $\theta^{(1)}$ from top to bottom for PVA corresponds to reactions with mouse anti-biotin antibodies at increasing probe concentrations of 27, 80, 240 and 480 nM.

For biotin-BSA conjugates, Type-1 sites (minority sites) have almost the same coverage of 0.3 to 0.4 regardless of biotin loading (biotin-BSA molar ratio during conjugation). The binding of the mouse anti-biotin antibodies at Type-1 sites

has a significantly larger K_D (6.6 to 32.1 nM) than that at Type-2 or majority sites (less than 0.15 nM), by almost 3 orders of magnitude. For biotin-PVA conjugates, we found similar results that the binding of the mouse antibodies at one of the two sites always had a very small K_D or equivalently small dissociation rate. The difference in K_D between Type-1 sites (22 to 41 nM) and Type-2 sites (less than 0.1 nM) was again as large as 3 orders of magnitude. We note that it is necessary to monitor the dissociation process for a long time given the signal-to-noise ratio in order to acquire an accurate measure for small dissociation rates, in addition to using two-site Langmuir reaction model.

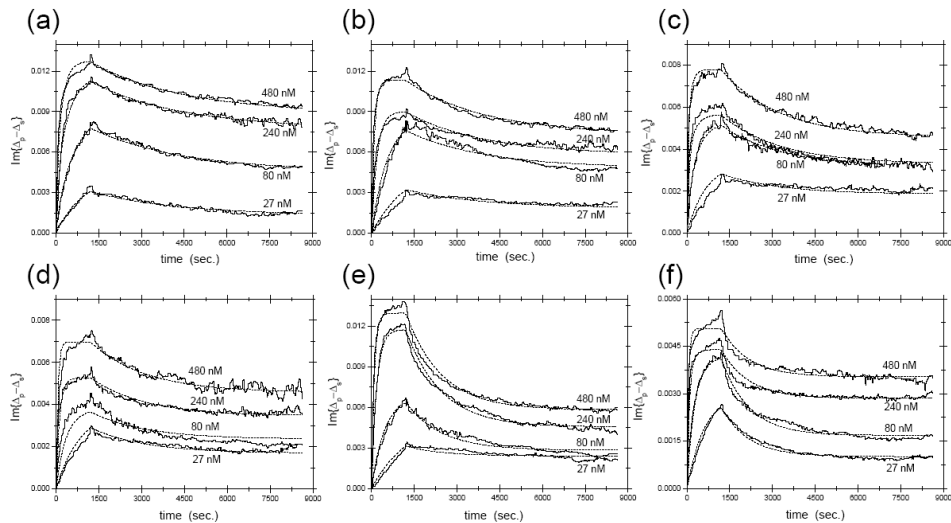


Fig. 5. Real-time binding curves of anti-biotin mouse antibodies reacting with surface-immobilized biotin conjugates: (a) 40× biotin-BSA; (b) 20× biotin-BSA; (c) 10× biotin-BSA; (d) 5× biotin-BSA; (e) 4% biotin-PVA; (f) 1% biotin-PVA. Probe concentrations of 480, 240, 80 and 27 nM were used. Each set of curves was fitted globally using a two-site Langmuir model for both association and dissociation (dotted line). Fitting parameters are listed in Table 1.

Table 1. Equilibrium dissociation constants K_D and other parameters of anti-biotin mouse antibodies reacting with surface-immobilized biotin-BSA and biotin-PVA conjugates. The parameters are derived from fitting 4 sets of binding curves in Fig. 5 using the two-site Langmuir reaction model.

	$\theta^{(1)}$	$k_{on}^{(1)}$ (Ms) ⁻¹	$k_{off}^{(1)}$ (s) ⁻¹	$K_D^{(1)}$ (nM)	$k_{on}^{(2)}$ (Ms) ⁻¹	$k_{off}^{(2)}$ (s) ⁻¹	$K_D^{(2)}$ (nM)
40×BSA	0.30	4.87×10^4	3.19×10^{-4}	6.55	9.80×10^3	$<9 \times 10^{-7}$	<0.092
20×BSA	0.35	2.10×10^4	3.69×10^{-4}	17.57	2.12×10^4	$<2 \times 10^{-6}$	<0.094
10×BSA	0.41	1.53×10^4	4.91×10^{-4}	32.09	6.96×10^4	$<3.6 \times 10^{-6}$	<0.052
5×BSA	0.34	4.12×10^4	5.25×10^{-4}	12.74	3.04×10^4	$<4.9 \times 10^{-6}$	<0.161
4%PVA	0.16 0.53 0.61 0.55	2.25×10^4	8.03×10^{-4}	35.69	2.04×10^4	$<1.9 \times 10^{-6}$	<0.093
2%PVA	0.27 0.61 0.58 0.39	3.67×10^4	8.14×10^{-4}	22.18	3.06×10^4	$<1 \times 10^{-6}$	<0.033
1%PVA	0.61 0.60 0.35 0.30	2.46×10^4	1.04×10^{-3}	40.81	6.31×10^4	$<7 \times 10^{-7}$	<0.011

4. CONCLUSIONS

We demonstrated two platforms for preparing small molecule microarrays using BSA and PVA as macromolecular scaffolds. Both molecules carry small molecules through conjugation and serve effectively as anchors to epoxy-functionalized glass slide surface. Since BSA and PVA are chemically inert in different ways, they are two choices when non-specific binding during subsequent protein binding assays on the small molecule microarrays is to be minimized. Using an OI-RD scanning microscope to detect end-points and real-time kinetics of protein binding reactions on a biotin microarray, we demonstrated that both BSA and amine-modified PVA platforms were efficient and viable for immobilization of small molecules in microarray-based assay application.

ACKNOWLEDGMENT

This work was supported by National Institutes of Health under R01-HG3827.

REFERENCES

- [1] Kuruvilla, F. G., Shamji, A. F., Sternson, S. M., Hergenrother and P. J., Schreiber, S. L., "Dissecting glucose signalling with diversity-oriented synthesis and small-molecule microarrays," *Nature* 416, 653-657 (2002).
- [2] Koehler, A. N., Shamji, A. F. and Schreiber, S. L., "Discovery of an inhibitor of a transcription factor using small molecule microarrays and diversity-oriented synthesis," *J. Am. Chem. Soc.* 125, 8420-8421 (2003).
- [3] Tolliday, N., Clemons, P. A., Ferraiolo, P., Koehler, A. N., Lewis, T. A., Li, X., Schreiber, S. L., Gerhard, D. S. and Eliasof, S., "Small molecules, big players: the National Cancer Institute's initiative for chemical genetics," *Cancer Res.* 66, 8935-8942 (2006).
- [4] Xu, Q., Miyamoto, S. and Lam, K. S., "A novel approach to chemical microarray using ketone-modified macromolecular scaffolds: Application in micro cell-adhesion assay," *Mol. Diversity* 8, 301-310 (2004).
- [5] Lee, M. and Shin, I., "Fabrication of chemical microarrays by efficient immobilization of hydrazide-linked substances on epoxide-coated glass surfaces," *Angew. Chem. Int. Ed. Engl.* 44, 2881-2884 (2005).
- [6] Bradner, J. E., McPherson, O. M. and Koehler, A. N., "A method for the covalent capture and screening of diverse small molecules in a microarray format," *Nature Protocols* 1, 2344-2352 (2006).
- [7] Kanoh, N., Kyo, M., Inamori, K., Ando, A., Asami, A., Nakao, A. and Osada, H., "SPR imaging of photo-cross-linked small-molecule arrays on gold," *Anal. Chem.* 78, 2226-2230 (2006).
- [8] Lam, K. S., Salmon, S. E., Hersh, E. M., Hruby, V. J., Kazmierski, M. and Knapp, R. J., "A new type of synthetic peptide library for identifying ligand-binding activity," *Nature* 354, 82-84 (1991).
- [9] Kodadek, T., "Protein microarrays: prospects and problems," *Chem. Biol.* 8, 105-115 (2001).
- [10] Sun, Y. S., Landry, J. P., Fei, Y. Y., Zhu, X. D., Luo, J. T., Wang, X. B. and Lam, K. S., "Effect of fluorescently labeling protein probes on kinetics of protein-ligand reactions," *Langmuir* 24, 13399-13405 (2008).
- [11] Azzam, R. M. A. and Bashara, N. M., [Ellipsometry and Polarized Light], North Holland Publication, Amsterdam (1987).
- [12] Landry, J. P., Zhu, X. D. and Gregg, J. P., "Label-free detection of microarrays of biomolecules by oblique-incidence reflectivity difference microscopy," *Opt. Lett.* 29, 581-583 (2004).
- [13] Zhu, X. D., "Oblique-incidence optical reflectivity difference from a rough film of crystalline material," *Phys. Rev. B.* 69, 115407 1-5 (2004).
- [14] Zhu, X. D., "Comparison of two optical techniques for label-free detection of biomolecular microarrays on solids," *Opt. Comm.* 259, 751-753 (2006).
- [15] Thomas, P., Nabighian, E., Bartelt, M. C., Fong, C. Y. and Zhu, X. D., "An oblique-incidence optical reflectivity difference and LEED study of rear-gas growth on a lattice-mismatched metal substrate," *Appl. Phys. A* 79, 131-137 (2004).
- [16] Landry, J. P., Sun, Y. S., Guo, X. W. and Zhu, X. D., "A study of protein reactions with surface-bound molecular targets using oblique-incidence reflectivity difference microscope," *Appl. Opt.* 47, 3275-3288 (2008).
- [17] Morton, T. A., Myszka, D. G. and Chaiken, I. M., "Interpreting complex binding kinetics from optical biosensors: A comparison of analysis by linearization, the integrated rate equation, and numerical integration," *Anal. Biochem.* 227, 176-185 (1995).